The 11th TSAE International Conference

26-27 April 2018

Available online at www.tsae.asia

Analysis of the Performance of Granular Material Flow in Bucket Elevator

Sathaphon Wangchai[1]*

[1]Department of Materials Handling and Logistics Engineering, Faculty of Engineering, King Mongkut's University of Technology North Bangkok, Bangsue, Bangkok, 10800, Thailand
*Corresponding author: Tel +66-8-8112-8778, Email: sathaphon.w@eng.kmutnb.ac.th

Abstract

Bucket elevator is the most common elevator used for the vertical transport. Currently, it was used in the rice mill and other granular materials; the capacity is an important factor in the choice of the conveyor. There are two parameters of the bucket conveyor need to be considered such as the rotational speed and level of the granular materials inside the bucket. This study was to examine the correlation of variables influencing the performance of the bucket capacity, material discharge behaviour, level of the materials in the bucket, installation distance of each bucket and level of the materials feed. The experiment was operated in the range between 70 - 130 RPM. The material discharge was recorded by the digital video camera to observe the bucket conveyor. In addition, this work illustrated the granular material model by using Discrete Element Method (DEM) is used to investigate the effects of bucket designs, operating parameters, granular material characterisation and to understand the mechanisms of granular interactions. Moreover, it was to predict the material volume inside the bucket. Finally, the results were validated in the stimulating with experimental data for ensuring the accuracy and development of the bucket elevator system.

Keywords: Bucket elevator, Discharge angle, Bucket design, Conveyor capacity, Discrete Element Method

1 Introduction

The handling, transport of bulk materials or granular materials movement from one to another location. The performance of the materials handling depends on the type of material handling, shape and size distribution of generated particles, physical and mechanical properties of the material are important for the design of the conveyor equipment.

Bucket elevators are designed to the granular or bulk solids material movement vertically. They are attached to an endless spliced loop of the belt which travels in a continuous fashion around the tail pulley from the boot section of an elevator, where the material feed to the bucket. The material in buckets moving up and over the head pulley where they are emptied into the material discharge out of the system and then the bucket moving back down to the boot section and continue the cycle. The centrifugal bucket elevator is the most commonly used vertical conveyors for the handling of material, for all types of free-flowing, powdered bulk solids such as agricultural seed, animal feed and more. The conveyor operates at high speeds which throw the materials out of the buckets into the discharge port by centrifugal force. The material feed to the buckets on the up leg side of the boot sections and the buckets frequently dig through the material during loading.

Discrete element modelling (DEM) is becoming an increasingly popular method for the simulation, analysis and visualisation of the behaviour of a grain or powder material flow and handling of bulk materials, and as such is used in a wide variety of models in the process engineering. The principle of DEM is to track each particle, in a time stepping simulation, the particle's trajectory, velocity, motion and rotation of individual particle element in a system to evaluate its position and orientation, and then to calculate the interactions between the elements themselves and also between the elements and their environment (Walls and other particles). Using calibrated material models, representative simulations of real-world problems can accurately be predicted. The properties of materials used in mathematical models include bulk density, solid density, shear modulus, Poisson's ratio, the coefficient of restitution, the coefficient of static friction, and coefficient of rolling friction. There are numerous studies on how to test (Gonzalez-Montellano, Llana et al. 2011) Include the size and shape of the sample material. DEM is therefore essential for calculating the particle's particle velocity, particle contact force, particle collision, mass flow rate and more. All of these events are not available in the laboratory to monitor the movement behaviour of the material at all times from the testing.

This study investigated the materials movement and discharge behaviour of paddy from the feeder with conveyor speed in the range of 130-70 rpm, and five different positions of the feed height measured

from the centre of the tail pulley of bucket elevator. Considering the fill volume of the material inside the bucket, which influenced the transfer rate and the material's discharge angle, and also predicted the movement behaviour of the material and behaviour of the materials discharged from the bucket at the head pulley using a Discrete Element Method (DEM). Finally, the results from the simulation of the particles movement will make a comparison with the results of the experimental.

2 The Discrete Element Method (DEM)

DEM is a numerical technique developed by Cundell and Strack (Cundall and Strack 1979) for predicting the behaviour of each particle translational and rotational motion of each particle, including collisions between each particle and between particles and boundaries. The dynamics method uses Newton's second law of motion and the force-displacement law (Cundall and Strack 1979) to determine the particle translational and rotational in a system. (Yang, Yu et al. 2008). The contact model used in DEM to the simulation of both particle-particle and particle-wall contacts was based on Hertz-Mindlin no-slip contact models (Cundall 1988) with spring-dashpot and frictional slider in the tangential direction (Tsuji Y., Tanaka T. et al. 1992). The equations are as follows.

$$m_i \frac{dv_i}{dt} = \sum_{j=1}^{k_i}(F_{ij}^n + F_{ij}^s) + m_i g \quad (1)$$

$$I_i \frac{d\omega_i}{dt} = \sum_{j=1}^{k_i}(R_i \times F_{ij}^s - \mu_r R_i |F_{ij}^n| \hat{\omega}_i) \quad (2)$$

Where m_i , I_i , v_i and ω_i are the mass, the moment of inertia, translational velocities and rotational velocities of particle i , respectively. F_{ij}^n , F_{ij}^s and $m_i g$ represent the normal contact force, the tangential contact force imposed on particle i by particle j and gravitational force, respectively. R_i represents a vector from the centre of particle to contact surface, μ_r represents the coefficient of rolling friction and $\hat{\omega}_i$ is a unit vector equal to ω_i divided by its magnitude. The magnitude of the normal force between two particles is given as:

$$F_n = -k_n \Delta x + C_n v_n \quad (3)$$

The magnitude of the tangential force is given as:

$$F_t = \min[\mu F_n, k_t \int v_t dt + C_t v_t] \quad (4)$$

where k_n and k_t are the normal stiffness and tangential stiffness respectively, Δx is the particle overlap, v_n and v_t are relative normal velocity and relative tangential velocity respectively, C_n and C_t are the normal damping coefficient and tangential damping coefficient respectively, C_n depends on the coefficient of restitution, e defined as the ratio of the normal component of the relative velocity after and before the collision.

$$C_n = -2\ln(e)\frac{\sqrt{m_{ij}k_n}}{\sqrt{\pi^2+ln^2(e)}} \quad (5)$$

$$m_{ij} = \frac{m_i m_j}{m_i+m_j} \quad (6)$$

where m_{ij} is the reduced mass of two particles i and particles j.

3 Material Properties Using in DEM

Materials properties input to EDEM simulations can be divided into two categories; material properties and interaction properties (Grima and Wypych 2011). Materials properties are Poisson's ratio, density and shear modulus. Interaction properties between each particle and particle/geometry are the coefficient of restitution, the coefficient of static friction and coefficient of rolling friction. Particle shape and particle size distribution also are modelled appropriately. Table 1 summarises the values of the material properties and the interaction materials.

The long grain of dry paddy is from the general market in Thailand. Dimensions of particle spheres are measured using a vernier calliper measuring the length (L), the width (W) and the thickness (T) of the seed and calculating the diameter of the spherical equivalent effective diameter (D_e) (Adebowale, Sanni et al. 2011) as shown in equation (7)

$$D_e = (LWT)^{1/3} \quad (7)$$

The Mass of the material is calculated from 100 seeds weighing of 2.6g, and the volume of the material is determined by the 100 seeds of material instead of the water and records the change of the volume water formed and the average per unit of material seeds.

Table 1: Materials Properties

Properties	Paddy	Steel
Particle volume (m^3)	1.4e-7	-
Particle mass (g)	0.026	-
Particle density (kg/m^3), (ρ_s)	1060	1000
Bulk density (kg/m^3), (ρ_b)	471.16	-
Poisson's ratio (ν)	0.25	0.45
Shear modulus (Pa), (G)	1e7	1e10
Coefficient of restitution,(e)	0.4548	0.5
Coefficient of static friction,(μ_s)	0.3	0.5
Coefficient of rolling friction,(μ_r)	0.01	0.01

The particle density (ρ_p) of a seed material is the mass divided by the true volume of the paddy. By taking weight-aware materials in place of known volumes, consider the change in volume of water. In the case of loosed-poured bulk density (ρ_b) is the ratio of the mass per unit volume of a paddy including the interstitial voids between the particles (Grima and Wypych 2011). In this work, the mass-volume ratio of the paddy was investigated by weighing a container of known volume without the paddy material and then gently pouring paddy into the container. The paddy were poured through conical hopper and allowed to fall a fixed height of 50 mm approximately to the cylindrical 1000 ml container. Excess paddy was removed using a ruler to scrape slowly across the top of the cylindrical container, without disturbing the particles settled loosely in the container (Wangchai, Hastie et al. 2013). In this case, five times are performed, based on the average.

The porosity of the material is the relationship between material density (ρ_s) and total material density (ρ_b) (Mohsenin 1986) It can be determined from equation (8)

$$P = \frac{1-\rho_b}{\rho_t} \times 100 \quad (8)$$

The particle coefficient of restitution (e)is defined as the ratio of the height of the particle after an impact to the height of the particle before impact using an experiment similar to that described by (Hastie, Grima et al. 2008). The e value was computed as the ratio of the square root of the height of the material after impact and rebound trajectories that were vertical (h_r) (particles not rotating) and the initial height of the material before falling to the ground (h_i). For this purpose 25 paddy seeds were dropped from a height of 250 mm onto a flat wall surface is consider the equation (9).

$$e = \sqrt{(h_r/h_i)} \quad (9)$$

The determination of the coefficient of friction (μ_s)between particle and wall ($\mu_{s(p.w)}$) was based on particles beginning to roll or slide on a tilting flat plate (Paddy plate and Steel plate square sheet). At this point, the experiment is stopped and the angle of inclination of the flat plane is measured to calculate the value of coefficient of friction ($\mu_{s(p.w)}$). Similar to other researchers (Hastie 2010), the coefficient of friction ($\mu_{s(p.p)}$) between the particles is approximated by DEM modelling to match the experiment inclination tester and calculate using equation (10).

$$\mu_s = \tan(\alpha) \quad (10)$$

when μ_s is the coefficient of frictional static and α is the angle that causes the starting material to move.

The coefficient of rolling friction (μ_r) between particles ($\mu_{r(p.p)}$), particle and wall ($\mu_{r(p.w)}$) is approximated in DEM modelling to match the experiment (Grima and Wypych 2011). Rolling resistance between particles was measured indirectly using the translating tube slump tester.

The angle of repose ($\propto$) is the angle of the slope surface formed when a quantity of paddy is poured into a cylindrical glass tube and then moving the glass tube in the vertical and shown a heap of paddy on the floor (Hastie, Grima et al. 2008). The material pile angle is determined by measuring the width of the pile base and the height of the piles of materials and calculating from equation (11). All the experiments were repeated five times for each paddy samples, and the average values were reported.

$$\propto = tan^{-1}\left[\frac{high\ of\ the\ heap}{(\frac{1}{2}) \times (wide\ of\ the\ heap)}\right] \quad (11)$$

The values in Table 1 were used to construct preliminary DEM models for the material. The particle shape and sizing of the paddy are shown in Figure 1. 100 paddy particles were selected at random from the bulk material to determine particle shape and particle size (Hastie, Grima et al. 2008). Measurements of 3 key particle dimensions were taken for each particle corresponding roughly to the particle length and two perpendicular diameters (Grima and Wypych 2011). The mean particle diameter was taken as the average of all the recorded dimensions: particle diameter (max and min) were 1.83, 2.47 mm respectively and particle length was 8.54 mm, with an equivalent effective diameter of 3.4 mm and the porosity is $\%60.37$, while the angle of repose is 35.83°. Therefore, the model of the paddy is composed of three spheres as described in previous paper (Wangchai and Tragoonsubtavee 2017), the volumes and weights are equivalent to the actual material, and material properties are shown in Table 1

Figure 1 Particle representation of the paddy; (a) Photo of paddy and (b) particles used in EDEM

The bucket elevator used in this works to determine the discharge behaviour of paddy is shown in Figure 2, with a height of 2 m and a volume of each

bucket, 9e-5 m^3, and the casing made from steel. There are three models separate by some buckets, 24, 30 and 40 are installed at a bucket pitch of 0.175 m, 0.14 m and 0.105 m, respectively. There are 5 levels of material feeding, as shown in Figure 2(a) the top Figure present the highest level (top level = 135 mm measured from the centre tail pulley to the height), middle level (centre tail pulley) and lowest level (135 mm measured from the centre tail pulley to the bottom). Figure 2(b) shown the bucket elevator model, seven speeds of the head pulley rotation consist of 70 rpm (1.356 m/s), 80 rpm (1.549 m/s), 90 rpm (1.743 m/s), 100 rpm (1.937 m/s), 110 rpm (2.131 m/s), 120 rpm (2.324 m/s) and 130 rpm (2.518 m/s). The materials feed at the boot section of the bucket elevator of 1.5 kg/s. Finally, record the materials discharged from the head pulley of the conveyor by high-speed camera mode.

4 Results

4.1 Comparison between experimental and simulation results

Figure 3 shows typical figures of the particle discharge at the head section for the experiments and the particle flow in simulation model different rotational speed, with the head pulley rotating clockwise and the same starting location for the particles feed at the top level (135 mm height).

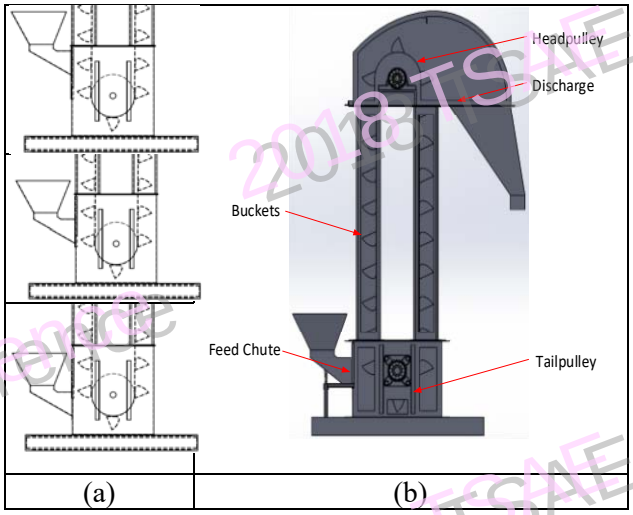

Figure 2 (a) position of the feed high; top row is the highest level, middle row is horizontal level and bottom row is lowest level (b) bucket elevator model

The results in the first column are from experiment and second column for DEM simulation. Each row is a different rotating speed of 70, 80, 90, 100, 110, 120 and 130 rpm. It can be seen that the material at the free surface begins to disperse from the first bucket with centrifugal force and moves along with the material next to the top surface. The material is moving out of the bucket at an angle of about 50°. The bottom part of the material starts moving from the surface of the bucket at a 90° to 120° angle. For the rotating speeds higher than 90 revolutions per minute, it shows that when the speed of the bucket increases. For speeds below 80 rpm, the material will discharge at higher than 140°.

The colour shows the particle velocity discharge at the head pulley of the bucket elevator of the paddy within the computer simulation. This is very difficult for the study of the particle movement in the experimental. Therefore a numerical method was performed to predict discharge of material behaviour by centrifugal force. The movement of the particle occurring the velocity on each particle by bucket elevator of the paddy within the computer simulation. It can be seen that when the speed of rotation of rises, the speed of material movement increases accordingly. This means that the force acting on the material increases due to the centrifugal force of the head pulley, materials were impacted on the wall at higher speeds.

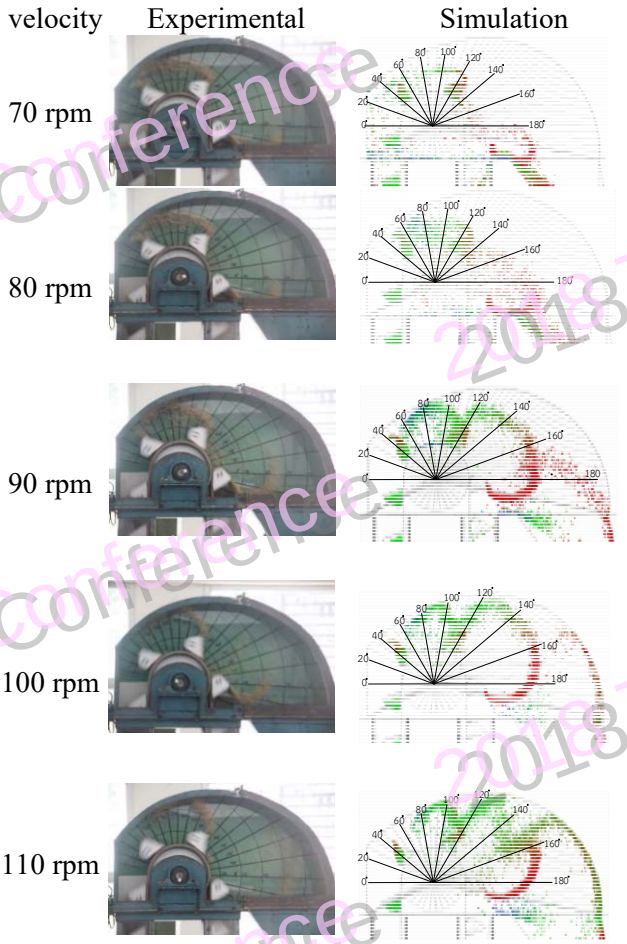

120 rpm

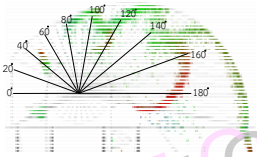

130 rpm

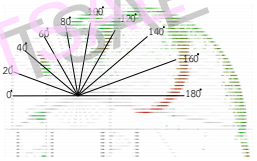

Figure 3 Comparison the materials discharge by experimental and simulation (colour image by the particle velocity)

4.2 Filling the buckets

The material in the bucket as the operating moving from the bottom up to the head elevator. The materials overflow from the edge of the bucket into the bottom until the materials inside the bucket is horizontal level, an average for one bucket from all the materials in bucket movement upward of the conveyor before throw out from the bucket at the head pulley. The fill volume of the material inside each bucket during the operation starting from the bottom to the top of the bucket elevator. There are five level of the material feed chute height include; 135 mm, 67.5 mm, 0 mm, -67.5 mm and -135 mm measured from the centre of the tail pulley, and the bucket variable of the head pulley speeds in the range from 70 to 130 rpm with material feed flow rate is 1.5 kg/s

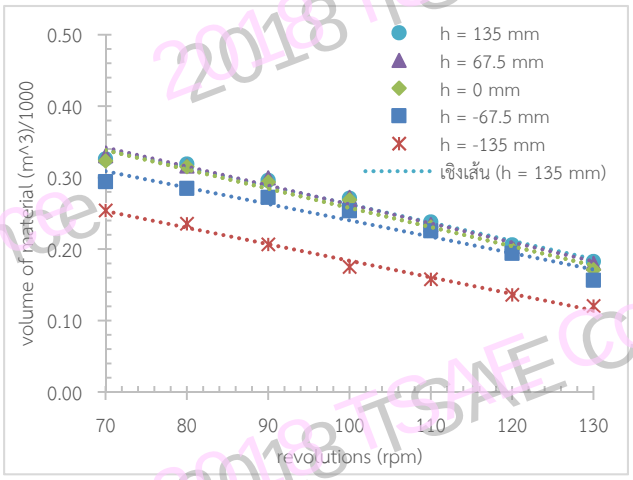

Figure 4 Shows the volume of material in the bucket and revolutions

It can be seen that the volume of material in the bucket was decrease when the rotational of the head pulley increases and the level of material feed decrease. For the head pulley rotational height speeds the bucket moving higher than the particle velocity feed to the system. While, lower speeds the particle in the bucket combine from the dig and feed chute section. It is found that at the higher levels, the amount of material in the bucket will be 1.5 times higher than the low level. As a result, it is unsuitable for the material transfer to the bucket as the high rotational speed.

Figure 5 shows the amount of material in the bucket of three levels consist; 135 mm, 0 mm, and 135 mm measured from the centre of the tail pulley, with 24, 30 and 40 buckets. It can be seen that the highest-level of the materials feed records the highest volume of materials in the bucket and decrease when the level of materials feed lower.

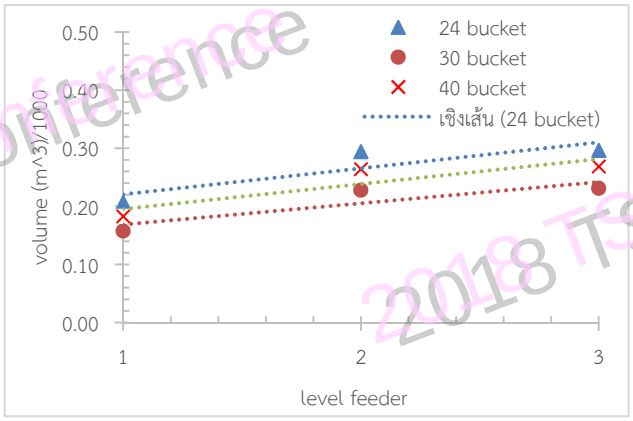

Figure 5 Shows the volume of material in the bucket (1=lowest level, 2=middle level, 3 = highest level, Figure 2a)

4.3 Centrifugal discharge

The material discharged from the head pulley of the bucket at the rotational speed 90 rpm shown in Figure 6. The simulation results in a different number of bucker, 24, 30 and 40 bucket and three level of the feed high were installed. The particle discharge from the bucket has two main flow behaviour consisting of the particle falling to the boot section of the bucket with the weight of the material to combine with the material at the boot section and another particle discharge from the head pulley by centrifugal force moves along the discharge path. The result is the material handling flow rate. In the course of releasing the material from the bucket, the inertia occurs with the material to deliver the material forward until it collides with the inner surface of the head elevator and falls to the bottom. The colour characteristics of the particle as shown in Figure 6 indicate the velocity of the particle. (Displayed in red or blue) moreover, the red particle's speed greater than 3 meters per second.

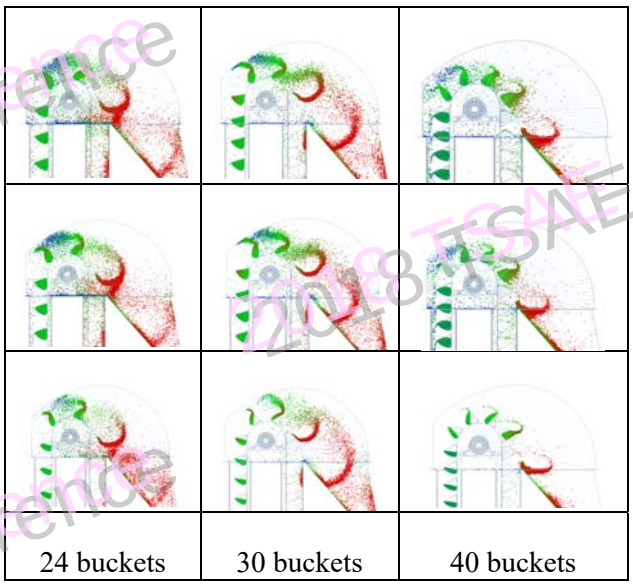

Figure 6 shown the particle discharge at 90 rpm, (top row at height level (+135 mm), middle row at the middle level (0 mm) and bottom row at the low level (-135 mm)) (colour image by the particle velocity)

4.4 Optimal Designs (material flow rate)

Level of materials feeds affected the amount of material in the bucket. Figure 7 to 9 shows the material flow rate per unit time (sec). There are five different level of material input; highest level to the lowest level as shown in Figure 2a, different coefficient of friction between each particle and a different number of the bucket were installed.

Figure 7, It shows that the high level has a higher material transfer rate than the low level of material feed of about 300 - 600 percent. Considering at the rotational speed increases more than 110 rpm, it is evident that the amount of material is reduced due to the materials movement in the bucket, the speed of the bucket affects to the amount of material in the bucket dropped. The material contained within the bucket comes from two components: the feeder level is low, the bucket was dig the material at the boot section of the bucket elevator, and only a lowest level small amount of material in the bucket provided from the feed chute. In the case of high-velocity of the bucket, the amount of material flow is not enough to fill the bucket.

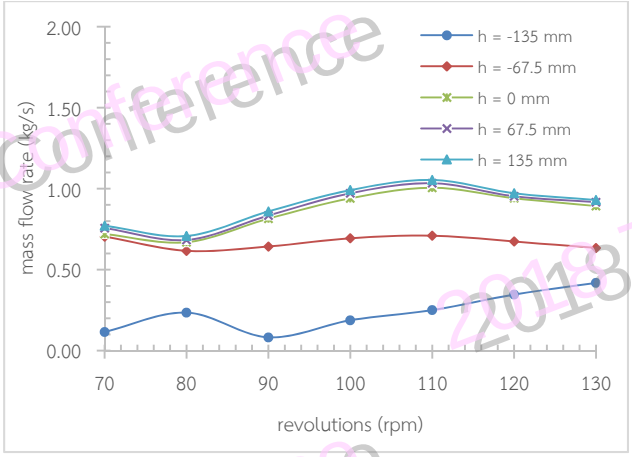

Figure 7 Shows the mass flow rate versus rotational speed and different high feed of material

Figure 8 indicates that the mass flow rate effect to the coefficient of the friction between particle and particle with various velocity in the rang 70 – 130 rpm. In can be seen that the mass flow rate increases the friction between particle and particle decreases. The mass flow rate slowly increases from the rotational speed of 80 rpm to 100 rpm and constant to the end time (130 rpm).

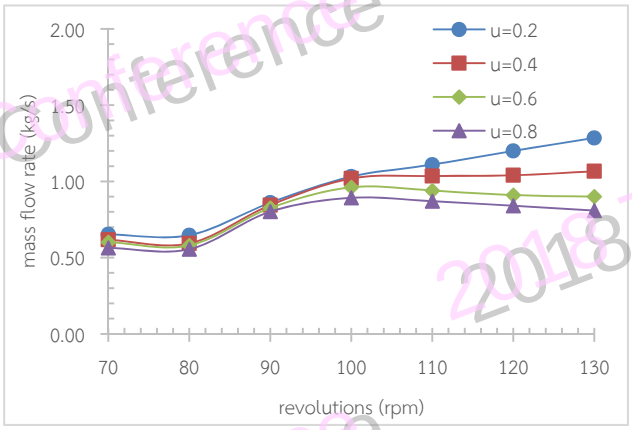

Figure 8 Shows the mass flow rate various revolutions and coefficient of friction each particle

5 Conclusion and Discussion

DEM simulation to determine the movement behaviour of each particle of material entering the bucket elevator until materials discharge from the head pulley of bucket elevator at the discharge port. Comparing the results will be a form of quantity. It can be seen from the image showing the discharge behaviour of the particle from the bucket at the head pulley through the outlet. By predicting the movement of the particle at different speeds. The accuracy of DEM simulation is based on the accuracy of the modelling variables as well as the size and shape of the model material, especially material properties.

The amount of particle moving entering to the bucket through the feed channel, at the maximum input flange (highest level) was higher than the minimum feeder (lowest level) with a difference of up to 600 percent, approximately. Due to the amount of material inside the bucket at the lowest level, it comes only from the bottom of the boot section. While the highest level is made up of two parts, the dig from the boot section and the delivery channel were combined. The rotating of the head pulley increase, the amount of material in the bucket will be reduced. Due to the inadequate flow of material into the bucket compared to the rotating velocity decrease for materials flow into the bucket. For the splatter behaviour of the material discharge at the head pulley of the conveyor through the discharge port. At higher speeds, the material will impact to the inside walls of the head elevator. At low speed, the material falls to the bottom by the weight of the material and spread on the head pulley of the drive shaft of the conveyor belt.

Finally, it was concluded that mathematical calculations for the behaviour of seed material by DEM method could be used for the analysis of conveyance behaviour of feed conveyor with centrifugal force or motion of material under the device and another conveyor.

6 Acknowledgment

This research was funded by Faculty of Engineering, King Mongkut's University of Technology North Bangkok

7 Reference

Adebowale, A.-R. A., L. O. Sanni, H. O. Owo and O. R. Karim (2011). "Effect of variety and moisture content on some engineering properties of paddy rice." Journal of Food Science and Technology 48(5): 551-559.

Cundall, P. A. (1988). Computer simulations of dense sphere assemblies**:** 113-123.

Cundall, P. A. and O. D. L. Strack (1979). "A discrete numerical model for granular assemblies." Geotechnique 29(1): 47-65.

Gonzalez-Montellano, C., D. F. Llana, J. M. Fuentes and F. Ayuga (2011). "Determination of the mechanical properties of corn grains and olive fruits required in DEM simulations." An ASABE Meeting Presentation

Grima, A. P. and P. W. Wypych (2011). "Discrete element simulations of granular pile formation." Engineering Computations: International Journal for Computer-Aided Engineering and Software **28**(3): 314-339.

Grima, A. P. and P. W. Wypych (2011). "Investigation into calibration of discrete element model parameters for scale-up and validation of particle–structure interactions under impact conditions." Powder Technology 212(1): 198-209.

Hastie, D. B. (2010). Belt conveyer transfers : quantifying and modelling mechanisms of particle flow. Dissertation/Thesis, University of Wollongong.

Hastie, D. B., A. P. Grima and P. W. Wypych (2008). Validated computer simulation modelling for complete conveyor transfer design. Conference Proceeding

Mohsenin, N. N. (1986). Physical properties of plant and animal materials. New York, N.Y, : Gordon and Breach Science.

Tsuji Y., Tanaka T. and Ishida T. (1992). "Lagrangian numerical-simulation of plug flow of cohesionless particles in a horizontal pipe." Powder Technology 71: 239-250.

Wangchai, S., D. B. Hastie and P. W. Wypych (2013). The Simulation of Particle Flow Mechanisms in Dustiness Testers. 11th International Conference on Bulk Materials Storage, Handling and Transportation, University of Newcastle, Australia, 2-4 July 2013.

Wangchai, S. and S. Tragoonsubtavee (2017). Performance of a bucket conveyor centrifugal escape center using DEM. The 31st Conference of Mechanical Engineering Network of Thailand, 4-7 July 2017, Phukhaongam Resort, Nakhonnayok, Thailand.

Yang, R. Y., A. B. Yu, L. McElroy and J. Bao (2008). "Numerical Simulation of Particle Dynamics in Different Flow Regimes in a Rotating Drum." Powder Technology 188(2): 170 - 170.